Identifying homoclinic orbits in the dynamics of intermittent signals through recurrence quantification

Vineeth Nair and R. I. Sujith

Citation: Chaos **23**, 033136 (2013); doi: 10.1063/1.4821475
View online: http://dx.doi.org/10.1063/1.4821475
View Table of Contents: http://chaos.aip.org/resource/1/CHAOEH/v23/i3
Published by the AIP Publishing LLC.

Identifying homoclinic orbits in the dynamics of intermittent signals through recurrence quantification

Vineeth Nair[a] and R. I. Sujith
Department of Aerospace Engineering, Indian Institute of Technology Madras, Chennai 600 036, India

(Received 9 May 2013; accepted 3 September 2013; published online 16 September 2013)

In this paper, we show how the phenomenon of intermittency observed in systems with turbulent flow-sound interaction is related to the formation of homoclinic orbits in the phase space. Such orbits that emerge via the intersection of the stable and unstable manifold of an equilibrium configuration result from interactions that happen at multiple spatial/temporal scales associated with turbulent convection and wave propagation. Through a quantification of the time spent by the dynamics in the aperiodic states using recurrence plots, we show how the presence of homoclinic orbits in the dynamics may be convincingly demonstrated, which is often not possible through a visual inspection of the phase space of the attractor. © *2013 AIP Publishing LLC*.
[http://dx.doi.org/10.1063/1.4821475]

The interaction of flow with sound can often lead to unsteady pressure fluctuations that display intermittent bursts, i.e., low amplitude, aperiodic oscillations embedded amongst higher amplitude periodic oscillations in a near-random manner. We show that these intermittent states give rise to homoclinic orbits in the phase space. These homoclinic orbits, which are often difficult to identify visually through phase space reconstruction, can be discerned by quantifying the recurrence properties of the system dynamics. We show that an exponential fall-off of the time spent by the dynamics in the aperiodic states provides an easy way of identifying homoclinic orbits in the underlying phase space.

I. INTRODUCTION

The phenomenon of intermittency has received a lot of attention in the description of deterministic dynamics arising from pattern forming complex systems. Through a study of simple dissipative dynamical systems, Pomeau and Manneville presented three models of intermittency classified as type I-III[1] to describe the routes of transition from a stable periodic behaviour to chaos. Even more varieties of intermittency were discovered later on such as chaos-chaos intermittency[2] (e.g., on-off intermittency[3] and in-out intermittency[4]), crisis-induced intermittency,[5] type-X intermittency,[6] or type-V intermittency.[7] There has also been a number of experimental observations[8,9] of intermittent dynamics in the literature.

Here, we present another dynamical system where intermittency is observed—that corresponding to the interaction of sound with turbulent flow. We study two systems that display intermittent oscillations as a result of sound-flow interaction, (i) a combustor with a bluff-body for flame stabilization, (ii) a pipe-tone whistler. The combustion chamber had a length of 700 mm, and a square cross-section of $90 \times 90\,mm^2$ with a bluff-body of 47 mm diameter for flame-stabilization. Further design details may be found in Nair *et al.*[10] The whistler consists of a duct of length 600 mm and diameter 50 mm terminated by a circular orifice of diameter 15 mm and thickness 5 mm. Similar configurations are described in Karthik *et al.*[11,12]

In the combustor, the acoustics of the confinement is driven mainly by the heat released through combustion adding energy into the turbulent flow and when there is a lock-in between the hydrodynamic fluctuations and the acoustics, large amplitude oscillations are established. In the whistler, pipe tone oscillations are set up when the vortex shedding frequencies at the duct exit match the natural acoustic frequencies of oscillations inside the duct. Here also, there is a lock-in between hydrodynamics and the acoustics of the confinement.

Shown in Fig. 1 are the unsteady pressure measurements made from the two systems whose dynamics is characterized by turbulent flow-sound interaction. Recently, Kabiraj and Sujith[13] showed that intermittency is possible in simple thermoacoustic systems prior to lean blowout of the flame. However, in their system, the intermittency was composed of high-amplitude chaotic oscillations that emerged from a quiet, laminar background. Here, we observe that the signals display what is termed an intermittent bursting phenomenon—bursts of periodic oscillations that appear in a near-random fashion amidst aperiodic irregular fluctuations. The dynamics of such systems can be thought of as being composed of two subsystems or attractors that operate on different time scales; acoustics which is characterized by the local speed of sound and hydrodynamics which is defined by the local flow speed. The current study aims to establish that such intermittent bursts arise naturally in systems composed of two attractors through the formation of homoclinic orbits in the phase space of the global system dynamics. It also aims, through analyzing the recurrence properties of these intermittent states, to provide a systematic way to inspect the

[a]Author to whom correspondence should be addressed. Electronic mail: v.vineeth.nair@gmail.com.

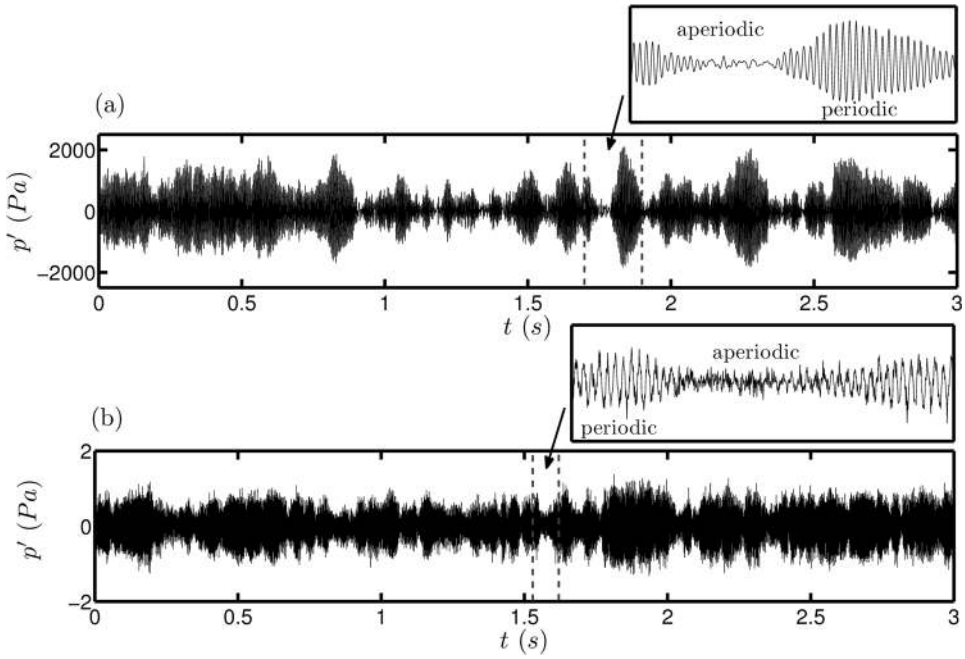

FIG. 1. Intermittent signals arising from sound-flow interaction. The time signals correspond to (a) unsteady pressure measurements made from a bluff-body stabilized combustor (90 mm from the backward-facing step) and (b) unsteady pressure measurements made from a pipe tone whistler (2 mm downstream of the orifice). The signals are composed of aperiodic, low-amplitude fluctuations interspersed amongst periodic, high amplitude fluctuations in a near random fashion. Notice that two signals differ by almost three orders of magnitude.

presence of such homoclinic orbits from a measured time signal.

II. INSPECTION OF HOMOCLINIC ORBITS

In order to understand the dynamical evolution of the measured variable and define measures that quantify homoclinicity, a reconstruction of the phase space of evolution is necessary. Since the amount of information available at the hands of an experimental researcher is limited and often is just the measurements of a single variable, techniques of delay embedding need to be employed to reconstruct the phase space, the procedure for which is outline below.

A. Phase space reconstruction

The dynamics of the system at different operating conditions can be visualized by reconstructing the phase space of evolution of the time signal acquired at those conditions.[14] In such a reconstruction, also known as delay-embedding, the measured time series is converted into a set of delay vectors that have one-to-one correspondence with one of the dynamic variables involved in the system dynamics. That is, we construct the vectors $\boldsymbol{p_i}(d) = \{p(t_i), p(t_i + \tau), p(t_i + 2\tau), \ldots, p(t_i + d - 1)\tau\}$ from the measured pressure data $p(t)$ such that these vectors in combination provide us with maximum information on the dynamics of the system. The elements of these vectors are the co-ordinates in the d-dimensional phase space of evolution of the time signal. To accomplish an appropriate reconstruction, we need to estimate the optimum time delay (τ_{opt}) for embedding the signal as well as the least embedding dimension (d_0) of the phase space composed of these delay vectors in which the dynamics unfold.

The optimum delay τ_{opt} is estimated as that first minimum of the average mutual information between the delay vectors.[15] The average mutual information of a time signal $p(t)$ is given by the expression

$$I(\tau) = \sum_{t=1}^{N} P(p(t), p(t+\tau)) \log_2 \left[\frac{P(p(t), p(t+\tau))}{P(p(t))P(p(t+\tau))} \right],$$

where, $P(E)$ represents the probability of occurrence of event E. Since average mutual information is an indicator of the amount of information shared by two data sets, the location of the minimum would, therefore, generate a set of delay vectors that would provide more information about the system than any of them in isolation.

To obtain a suitable embedding dimension d_0, we use the technique developed by Cao.[16] The method is an optimized version of the False Nearest Neighbors method[15] wherein one tracks the fraction of false neighbors in the phase space as the embedding dimension is progressively increased. A false neighbor in phase space changes its relative position with respect to its neighbouring points when the embedding dimension is increased. Mathematically, we can construct a measure $a(i, d)$ of the form

$$a(i,d) = \frac{||\boldsymbol{p}_i(d+1) - \boldsymbol{p}_{n(i,d)}(d+1)||}{||\boldsymbol{p}_i(d) - \boldsymbol{p}_{n(i,d)}(d)||},$$

where $i = 1, 2, \ldots, (N - d\tau)$ and $n(i, d)$ is the index of the nearest neighbour to the point $\boldsymbol{p_i}$. The dependency on the index i is removed by averaging $a(i, d)$ for different values of i as

$$E(d) = \frac{1}{N - d\tau_{opt}} \sum_{i=1}^{n-d\tau_{opt}} a(i,d).$$

Here, $E(d)$ is a function only of the dimension d and the optimum time lag τ_{opt}. The variation of $E(d)$ on increasing the dimension from d to $d + 1$ is determined by defining a measure $E_1(d)$ as

$$E_1(d) = \frac{E(d+1)}{E(d)}.$$

If $E_1(d)$ stops changing for values of d greater than $d_0 - 1$, then d_0 is chosen as the least embedding dimension for the time signal. Since the acquired time signal is limited, it is often difficult to distinguish a stochastic signal from a deterministic signal merely by observing the variations in $E_1(d)$. This is because although $E_1(d)$ saturates beyond a value of d for a deterministic signal, it is always increasing with d for random signals. To clearly distinguish deterministic signals from stochastic signals, an additional measure $E_2(d)$ can be defined as

$$E_2(d) = \frac{E^*(d+1)}{E^*(d)},$$

where

$$E^*(d) = \frac{1}{N - d\tau_{opt}} \sum_{i=1}^{N-d\tau_{opt}} |p(i + d\tau_{opt}) - p(n(i, d) + d\tau_{opt})|.$$

Since future values are independent of past values for random signals, $E_2(d)$ is independent of d and equals 1 for all values of d. For deterministic signals, since $E_2(d)$ is dependent on d, there must exist some values of d for which $E_2(d)$ is not equal to 1.

The average mutual information and the measures to obtain optimum dimension of embedding of the two unsteady pressure signals presented in Fig. 1 are shown in Fig. 2. The signals were acquired at a sampling rate of 10 kHz for a duration of 3 s. The optimum delay of embedding was estimated from the first minimum of the average mutual information of the two signals as $\tau_{opt} = 1.0$ ms and $\tau_{opt} = 0.5$ ms, respectively. The embedding dimension of the two signals showed no significant variation after $d = 9$ and hence the embedding dimension was safely chosen to be $d_0 = 10$. In the calculation of the embedding dimension, the last 5000 points (data for 0.5 s) of the signal were used. After reconstructing the phase space, recurrence properties of the intermittent signals were explored using recurrence plots.

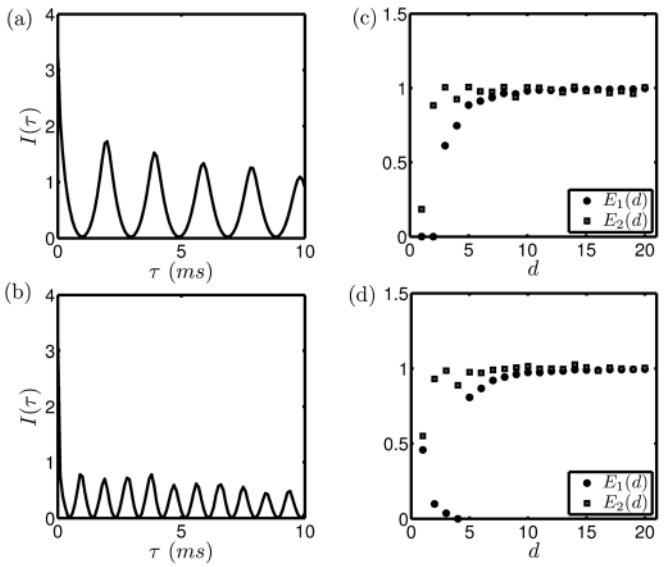

FIG. 2. Details of phase space reconstruction of the unsteady pressure signals from the combustor and the whistler during intermittency. The optimum delay for embedding was estimated from the first minimum of average mutual information I as (a) $\tau_{opt} = 1.0$ ms and (b) $\tau_{opt} = 0.5$ ms for the two signals, respectively. The values of the measures $E_1(d)$ and $E_2(d)$ for the two signals are plotted in (c) and (d). The embedding dimension was chosen to be $d_0 = 10$ for both the signals as there was no significant variation discernible past $d = 9$.

B. Recurrence quantification

The temporal features of the dynamics can be better understood by tracking the regularity of the trajectories using recurrence plots.[17] Recurrence is a fundamental property of dynamical systems and recurrence plots allow one to visually identify the times at which the trajectory of the system visits roughly the same area in the phase space. Recurrence plots are constructed by computing the pairwise distances between points in the reconstructed phase space and estimating a binary recurrence matrix R_{ij} in the following fashion:

$$R_{ij} = \Theta(\epsilon - \| p_i - p_j \|), \; i, j = 1, 2, \ldots, N - d_0\tau_{opt},$$

where Θ is the Heaviside step function and ϵ is a threshold or the upper limit of the distance between a pair of points in the phase space to consider them as close or recurrent. The indices represent the various time instances when the distances are computed. Recurrence plot is merely a plot of the symmetric matrix R_{ij} for various values of i and j (time instants). The elements of R_{ij} are just 1 s and 0 s which are then marked as black and white. The black points correspond to those time instants when the distance measured is less than ϵ. The time instants when the distance exceeds ϵ are marked as white.

The recurrence plots for a portion of the unsteady pressure signals are plotted in Fig. 3. The black patches represent the times at which the system lingers around the stable fixed point (distances less than the threshold) and the white patches represent the unstable oscillatory regimes (when the pairwise distances exceed ϵ). The recurrence plots were computed for 0.6 s of data, so that the intermittent bursts from low-to-high amplitudes and back are captured in the time interval.

The recurrence plots display a pattern with black squares and rectangles inside a lightly shaded structure. This can be a pattern characteristic of type-II or type-III intermittency.[18] Type-II intermittency happens near a Hopf bifurcation whereas type-III intermittency arises near a subcritical period doubling bifurcation. The nature of intermittency in the signal from the whistler was identified as type-III since the black patches in the recurrence plot have a rounded upper right corner. Also, period-2 oscillations were always observed at the onset of oscillations. The nature of intermittency could not be discerned from the recurrence plot (as type-II or type-III) for the signal from the combustor. However, we wish to point out that period-2 oscillations were observed in portions of the signal post the onset of periodic oscillations in the combustor. This leads us to suspect that the intermittency observed in combustors is also of type-III.

Although a close association between homoclinicity and intermittency has been shown experimentally,[19–21] identification of homoclinic orbits from a measured time series has proved a difficult task.

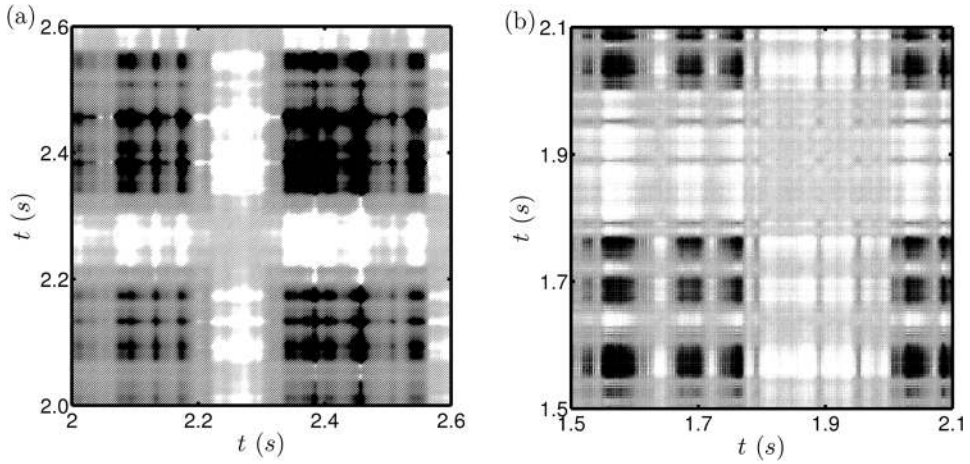

FIG. 3. Recurrence plots for 0.6 s from the (a) combustor and the (b) whistler time signals during intermittency. The threshold value of the ball was taken to be $\epsilon = 0.25D$, where D is the size of the attractor (length of the largest vector in phase space). In these plots, we see black squares and rectangles inside a lightly shaded structure. Intermittency in the whistler signal can easily be identified to be of type-III from the rounded shape of the upper right corners of rectangles of black patches. The recurrence plot of the combustor signal shows patterns that could emerge from type-II or type-III intermittency. However, the presence of period-2 oscillations in the signal post the transition to periodic oscillations suggests that the intermittency is of type-III.

C. Homoclinic orbits

A homoclinic orbit is one in which the unstable manifold of a hyperbolic equilibrium state of the system merges with its own stable manifold. In Fig. 4, the evolution in phase space of an intermittent burst is shown for the two signals. For the signal from the combustor, such a homoclinic orbit is visible in the reconstructed phase space that transitions the system dynamics from low amplitude chaos to high amplitude oscillations and back. The signal is seen to spiral out of the center to the unstable orbit and then spirals back in through the plane of oscillations. However, for the pressure signal from the whistler, the homoclinic orbit, is not seen; i.e., its existence cannot be inferred by a mere visual inspection of the phase space. Therefore, we propose a new technique to infer the presence of homoclinic orbits in the phase space of the global attractor.

The circulation time of trajectories in phase space for homoclinic orbits are dominated by their passage time near the saddle fixed point. This time is highly sensitive to external perturbations and the distribution of passage times for a given initial distribution of points near the saddle point is given by the expression[22]

$$P(T) = 2\lambda\Delta(T)e^{-\Delta^2(T)}/\sqrt{\pi}(1 - e^{-2\lambda T}),$$

where $\Delta(T) = \delta\left[\left(\frac{\alpha^2}{\lambda}\right)(e^{2\lambda T} - 1)\right]^{-1/2}$, λ is the unstable eigenvalue of the saddle point, α is the noise level rms, and δ is the size of the neighbourhood influenced by noise. $P(T)$ is a skewed distribution with its peak value different from the mean and has an exponential tail[22] as $T \to \infty$ ($P(T) \approx \frac{2\delta}{\sqrt{\pi\alpha}}\lambda^{\frac{3}{2}}e^{-\lambda T}$). This behaviour is independent of the details

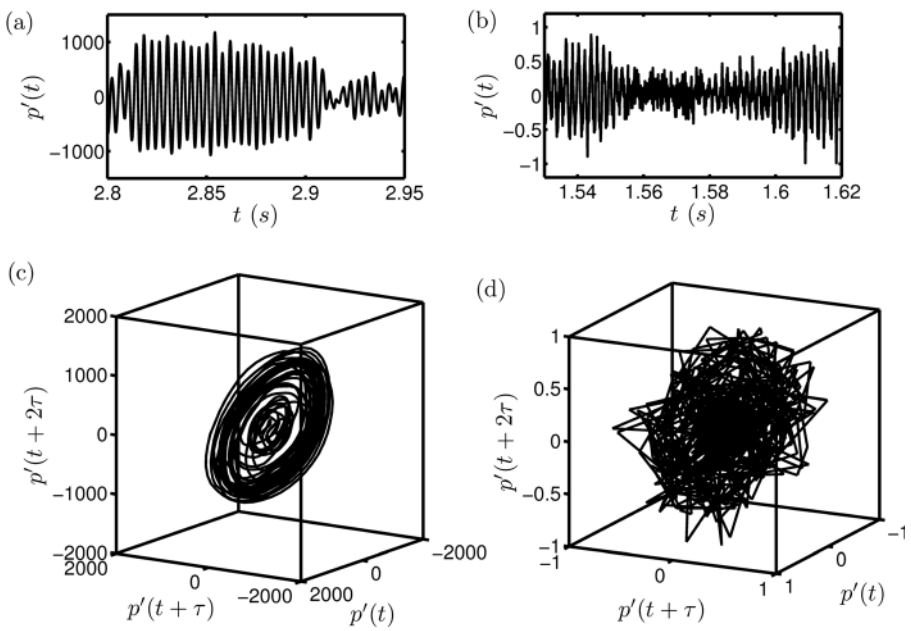

FIG. 4. Phase portraits (in 3 d) of a part of the (a) combustor and the (b) whistler time signals during intermittency are shown in (c) and (d), respectively. The embedding dimension was chosen to be $d_0 = 10$ for both the signals with $\tau_{opt} = 1.0$ ms and $\tau_{opt} = 0.5$ ms, respectively, for the two signals. The evolution of burst oscillations in phase space results in the aperiodic oscillations spiraling out into high amplitude oscillations and then again spirals back into the low amplitude aperiodic. Whereas such a homoclinic orbit is visible though barely in the phase plot of the combustor pressure signal, it is completely masked in the phase plot of the pressure signal from the pipe-tone whistler.

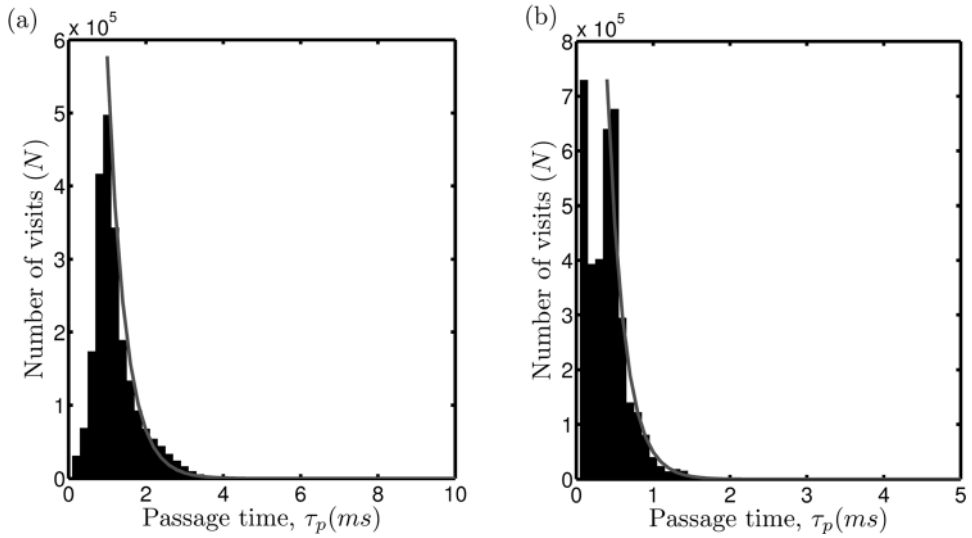

FIG. 5. Histograms of the frequency of visits as a function of the duration of time spent trapped in the low amplitude aperiodic regimes for (a) the combustor and (b) the whistler time signals during intermittency. The data set correspond to the first 7500 points for the whistler (sampled at 0.2 τ_{opt}) and an undersampled set for the combustor with 7500 data points (at a sampling rate of 0.2 τ_{opt} for the sake of comparison). A skewed distribution with an exponential fall-off is visible in both the histograms, which is a distinctive feature of systems that have homoclinic orbits in the phase space of dynamics. The whistler signal has some corruption for very small trapping time because the amplitudes are comparable to the noise levels in the measuring instrument. An exponential fit to the tail is shown as gray lines over the histogram.

of the initial distribution.[23] It is known that the distribution of the laminar phases (quiet, aperiodic regimes) for both type-II and type-III intermittencies have an exponential tail.[18] Thus, the analysis shows that systems exhibiting type-II or type-III intermittency are characterized by homoclinic orbits in the underlying phase space.

The distribution of the passage time of the dynamics in low amplitude regimes can be estimated from a recurrence plot as the frequency distribution of the vertical lines (or horizontal lines since the matrix is symmetric) in the recurrence plot. Histograms of this vertical length frequency distribution for the two signals were plotted in Fig. 5 to understand the variation of the visitation frequency as a function of the trapping time. The histogram reveals a skewed distribution with its peak off the mean and has an exponentially decaying tail.

The presence of such an exponential tail is thus indicative of homoclinic orbits in the system.[24] The trajectory of such a homoclinic orbit is repeatedly injected near the stable manifold of a saddle node as a result of the perturbations in the turbulent base flow. Hence, even for the case of the whistler signal (Fig. 5(b)), the skewed distribution with an exponential fall-off is clearly visible. The higher concentration at low passage times is because the fluctuations become comparable to the least count of the pressure transducer. Nevertheless, recurrence quantification serves as an efficient tool for the inspection of homoclinicity in the phase space of the system dynamics.

III. CONCLUDING REMARKS

Intermittent bursts characterized by periodic high amplitude oscillations amidst irregular low amplitude chaotic fluctuations are produced when a turbulent flow interacts with the acoustics of a confinement. Recurrence plots provide a convenient and quantitative descriptive tool to inspect and identify the presence of a homoclinic orbits in the underlying phase space by measuring the amount of time the system lingers around the low amplitude fluctuations. A skewed distribution of passage times with an exponential tail is a distinctive signature of systems with a homoclinic orbit; i.e., the trajectory is repeatedly injected near the stable manifold of a saddle in the presence of small perturbations. It seems thus possible that large-scale vortices often observed at the onset of periodic oscillations are intimately linked to the presence of such homoclinicity in the underlying dynamics.

ACKNOWLEDGMENTS

We would like to express our gratitude to Mr. T. Gireeshkumaran and Ms. A. Aanveeksha for their help in arranging the experimental setups. The design of the combustor was adapted from a swirl combustor configuration in TU Munich and we wish to thank Professor Wolfgang Polifke and Mr. Thomas Komarek for sharing the details of the design. The study was funded by Department of Science and Technology, Govt. of India.

[1]Y. Pomeau and P. Manneville, Commun. Math. Phys. **74**, 189 (1980).
[2]E. Ott, *Chaos in Dynamical Systems* (Cambridge University Press, New York, 1993).
[3]E. Ott and J. C. Sommerer, Phys. Lett. A **188**, 39 (1994).
[4]E. Covas, R. Tavakol, P. Ashwin, A. Tworkowski, and J. Brooke, Chaos **11**, 404 (2001).
[5]C. Grebogi, E. Ott, F. Romeiras, and J. A. Yorke, Phys. Rev. A **36**, 5365 (1987).
[6]T. J. Price and T. Mullin, Physica D **48**, 29 (1991).
[7]M. Bauer, S. Habip, D. R. He, and W. Martienssen, Phys. Rev. Lett. **68**, 1625 (1992).
[8]P. H. Hammer, N. Platt, S. M. Hammel, J. F. Heagy, and B. D. Lee, Phys. Rev. Lett. **73**, 1095 (1994).
[9]F. Argoul, J. Huth, P. Merzeau, A. Arneodo, and H. L. Swinney, Physica D (Amsterdam) **62**, 170 (1993).
[10]V. Nair, G. Thampi, S. Karuppusamy, S. Gopalan, and R. I. Sujith, "Loss of chaos in combustion noise as a precursor of impending combustion instability," Int. J. Spray Comb. Dyn. (to appear).

[11]B. Karthik, S. R. Chakravarthy, and R. I. Sujith, J. Acoust. Soc. Am. **113**, 3091 (2003).
[12]B. Karthik, S. R. Chakravarthy, and R. I. Sujith, Int. J. Aeroacoust. **7**, 321 (2008).
[13]L. Kabiraj and R. I. Sujith, J. Fluid Mech. **713**, 376 (2012).
[14]F. Takens, Lect. Notes Math. **898**, 366 (1981).
[15]H. D. I. Abarbanel, R. Brown, J. J. Sidorowich, and L. Tsimring, Rev. Mod. Phys. **65**, 1331 (1993).
[16]L. Cao, Physica D **110**, 43 (1997).
[17]N. Marwan, M. C. Romano, M. Thiel, and J. Kurths, Phys. Rep. **438**, 237 (2007).
[18]K. Klimaszewska and J. J. Zebrowski, Phys. Rev. E **80**, 026214 (2009).
[19]P. Richetti, F. Argoul, and A. Arneodo, Phys. Rev. A **34**, 726 (1986).
[20]H. Herzel, P. Plath, and P. Svensson, Physica D **48**, 340 (1991).
[21]D. Parthimos, D. H. Edwards, and T. M. Griffith, Phys. Rev. E **67**, 051922 (2003).
[22]P. Holmes, in *Whither Turbulence? Turbulence at the Crossroads*, edited by J. Lumley (Springer-Verlag, 1990), p. 195.
[23]E. Stone and P. Holmes, Phys. Lett. A **155**, 29 (1991).
[24]E. Stone, M. Gorman, M. El-Hamdi, and K. A. Robbins, Phys. Rev. Lett. **76**, 2061 (1996).